

## MHD Flow of Thixotropic Fluid with Variable Thermal Conductivity and Thermal Radiation

Tasawar HAYAT<sup>1</sup>, Sabir Ali SHEHZAD<sup>1,\*</sup> and Saleem ASGHAR<sup>2</sup>

<sup>1</sup>Department of Mathematics, Quaid-i-Azam University, Islamabad 44000, Pakistan

<sup>2</sup>Department of Mathematics, CIIT, ChakShahzad, Park Road, Islamabad 44000, Pakistan

(\*Corresponding author; e-mail: ali\_qau70@yahoo.com)

Received: 18 December 2011, Revised: 13 January 2012, Accepted: 11 January 2013

### Abstract

An analysis has been carried out to examine the two-dimensional and magnetohydrodynamic (MHD) flow of thixotropic fluid over a stretched surface. The thermal radiation effect in the heat transfer is considered when the thermal conductivity is not constant. Conservation of mass, momentum and energy leads to the governing partial differential equations of the present study. The resulting equations are solved for convergent series solutions. Numerical values of the skin-friction coefficient are presented and analyzed.

**Keywords:** MHD flow, thixotropic fluid, thermal radiation, variable thermal conductivity, stretching surface

### Introduction

In recent times, the dynamics of non-Newtonian fluids has become more and more important for industrial and engineering applications. The applications of non-Newtonian fluids are significant in micro/nano fluidic, biofluid and hematology, bacteriology, building and confectionery industries, chemical/petroleum engineering and mineral processing industries, bubble columns, polymer solution and food industries [1]. Due to diversity in behavior of the stress in the momentum equations, several models are suggested. The resulting equations for non-Newtonian fluids are complex, higher order and more nonlinear than the well known Navier-Stokes equations for viscous fluids. Some salient features of these fluids like shear thinning/shear thickening and relaxation and retardation time effects have already been studied in recent works [2-9].

The boundary layer flow over a stretching sheet with heat transfer has importance in the polymer industry. In particular, non-Newtonian fluids are quite common in polymer sheet extrusion from dyes, optical fibers, manufacturing processes, drawing of plastic films and many other

processes. In industrial processes involving such fluids, the quality of the final product is closely associated with the rate of cooling. The quality of such a sheet is affected by heat transfer between the sheet and the fluid [10-15].

Many materials in our daily life including drilling muds, cosmetic products, clay, suspension etc become less viscous with time. To explore the rheological properties of such types of materials, a thixotropic fluid model is more appropriate. A hysteresis influence is noticed when the shear rate of the thixotropic fluid is ramped up or down. Recently Sadeqi *et al.* [16] investigated the Blasius flow of thixotropic fluid. They analyzed the results numerically using the Newtonian-Kontorovitch method. The magnetohydrodynamic (MHD) flow with heat transfer are very important in magnetohydrodynamic power generators and accelerators, cooling of nuclear reactors, crystal growth etc. Several investigators analyzed the MHD flow under various conditions. Hayat *et al.* [17] reported the transient flow of viscoelastic fluid in the presence of a magnetic field. Magnetohydrodynamic flow of viscous fluid near

a stagnation point was addressed by Rashidi and Erfani [18]. They also considered the heat transfer phenomenon and analyzed the results analytically. Turkylmazoglu [19] studied the time-dependent MHD flow of viscous fluid by taking variable viscosity. MHD transient flow of dusty fluid was investigated by Makinde and Chinyoka [20]. The Navier slip condition and variable physical properties are also discussed in this study. Abbasbandy and Hayat [21] reported the MHD Falkner-Skan flow of viscous fluids by adopting the homotopy analysis method. Very recently, Soret and Dufour the effects on MHD peristaltic flow of viscous fluid were examined by Hayat *et al.* [22]. They obtained the results by a perturbation technique.

All the above investigations have been carried out by considering constant thermal conductivity. But it has now been proved that the thermal conductivity varies linearly with temperature from 0 to 400 °F [23]. Having such in mind, Vyas and Rai [24] investigated the boundary layer flow of viscous fluid with variable thermal conductivity. Furthermore, the thermal radiation effects are important in many industrial processes which involve heat transfer from nuclear fuel debris, underground disposal of radioactive waste material, storage of food stuffs and many others. Motivated by such facts, the present work is proposed to analyze the thermal radiation effects

on MHD flow of thixotropic fluid with variable thermal conductivity. The structure of this paper is as follows. In section 2, the mathematical model is formulated. Section 3 addresses the series solutions by adopting the homotopy analysis method (HAM) [25-30]. Convergence analysis and discussion of the results are presented in section 4. Section 5 has the final remarks.

### Basic equations

Consider a Cartesian coordinate system such that  $x$ -axis is along the stretched surface and  $y$ -axis is perpendicular to it. We consider the magnetohydrodynamic boundary layer flow of thixotropic fluid. A constant magnetic field of strength  $\mathbf{B}_0$  is exerted in the  $y$ -direction. The flow is steady and the magnetic Reynolds number is taken to be small so that an induced magnetic field is negligible in comparison to the applied magnetic field. The temperature of the surface ( $T_w$ ) is greater than the temperature of ambient fluid ( $T_\infty$ ). Heat transfer analysis is set up in the presence of thermal radiation and with variable thermal conductivity. Taking into account the Rosseland's approximation for radiative heat flux [24] mass, momentum and energy conservations are simplified as follows:

$$\frac{\partial u}{\partial x} + \frac{\partial v}{\partial y} = 0, \quad (1)$$

$$u \frac{\partial u}{\partial x} + v \frac{\partial u}{\partial y} = \nu \left( \frac{\partial^2 u}{\partial y^2} \right) - \frac{6R_1}{\rho} \left( \frac{\partial u}{\partial y} \right)^2 \left( \frac{\partial^2 u}{\partial y^2} \right) - \frac{\sigma^* B_0^2}{\rho} u + \frac{4R_2}{\rho} \left( \frac{\partial u}{\partial y} \right) \left( \frac{\partial^2 u}{\partial y^2} \right) \left( u \frac{\partial^2 u}{\partial x \partial y} + v \frac{\partial^2 u}{\partial y^2} \right) + \left( \frac{\partial u}{\partial y} \right)^2 \left( u \frac{\partial^3 u}{\partial x \partial y^2} + v \frac{\partial^3 u}{\partial y^3} + \frac{\partial u}{\partial y} \frac{\partial^2 u}{\partial x \partial y} + \frac{\partial v}{\partial y} \frac{\partial^2 u}{\partial y^2} \right), \quad (2)$$

$$\rho C_p \left( u \frac{\partial T}{\partial x} + v \frac{\partial T}{\partial y} \right) = \frac{\partial}{\partial y} \left( k \frac{\partial T}{\partial y} \right) + \frac{16\sigma T_\infty^3}{3k^*} \frac{\partial^2 T}{\partial y^2}, \quad (3)$$

where  $(u, v)$  are the velocity components parallel to the  $x$ - and  $y$ -axes.  $R_1$  and  $R_2$  are the constants,  $\nu$  the dynamic viscosity of the fluid,  $\rho$  the density of fluid,  $\sigma^*$  the electrical conductivity,  $T$  the temperature,  $k$  the variable thermal conductivity,  $C_p$  the specific heat,  $\sigma$  the Stefan-Boltzmann constant and  $k^*$  the mean absorption coefficient.

Eqs. (1) - (3) have to be solved subject to the boundary conditions

$$\begin{aligned} u &= u_w = cx, \quad v = -v_0, \quad T = T_w(x) = T_\infty + Dx^\alpha \quad \text{at } y = 0, \\ u &\rightarrow 0, \quad T \rightarrow T_\infty \quad \text{as } y \rightarrow \infty \end{aligned} \quad (4)$$

in which  $c$  is the stretching rate. We introduce the following change of variables

$$u = cxf'(\eta), \quad v = -\sqrt{c\nu}f(\eta), \quad \eta = y\sqrt{\frac{c}{\nu}}, \quad \theta(\eta) = \frac{T - T_\infty}{T_w - T_\infty}, \quad (5)$$

where prime denotes the differentiation with respect to  $\eta$  and we consider  $T_w(x) = T_\infty + Dx^\alpha\theta(\eta)$  at  $\eta = 0$  and variable thermal conductivity  $k = k_\infty[1 + \varepsilon\theta]$ ,  $k_\infty$  is the fluid free stream conductivity and  $\varepsilon$  is given by

$$\varepsilon = \frac{(k_w - k_\infty)}{k_\infty}. \quad (6)$$

The incompressibility condition is automatically satisfied by Eq. (5) and Eqs. (2)-(4) become

$$\begin{aligned} f''' + ff'' - f'^2 + K_1(x)f''^2f''' + K_2(x)(ff''^2f''' + f'^4 - ff''f''^2 - ff''^2f^{iv}) \\ - M^2f' = 0, \end{aligned} \quad (7)$$

$$(1 + \varepsilon\theta)\theta'' + \varepsilon\theta'^2 + \frac{4}{3}N\theta'' = \text{Pr}[\alpha\theta f' - f\theta'], \quad (8)$$

$$\begin{aligned} f = S, \quad f' = 1, \quad \theta = 1 \quad \text{at } \eta = 0, \\ f' \rightarrow 0, \quad \theta \rightarrow 0 \quad \text{as } \eta \rightarrow \infty. \end{aligned} \quad (9)$$

Here the non-Newtonian parameters are  $K_1(x) = -\frac{6R_1c^3x^2}{\rho\nu^2}$  and  $K_2(x) = \frac{4R_2c^4x^2}{\rho\nu^2}$ ,  $M = \sigma^*B_0^2 / \rho c$  the

Hartman number,  $S = v_0 / \sqrt{c\nu}$  the suction parameter,  $\text{Pr} = \frac{\rho C_p \nu}{k_\infty}$  the Prandtl number and  $N = \frac{4\sigma T_\infty^3}{kk_\infty}$  the radiation parameter.

The dimensionless form of the skin friction coefficient is

$$\text{Re}_x^{1/2} C_f = f''(0) - K_1 / 6[f''(0)]^3. \quad (10)$$

**Series solutions**

The homotopic solutions for  $f$  and  $\theta$  in a set of base functions

$$\{\eta^k \exp(-n\eta), k \geq 0, n \geq 0\} \quad (11)$$

can be expressed as

$$f(\eta) = a_{0,0}^0 + \sum_{n=0}^{\infty} \sum_{k=0}^{\infty} a_{m,n}^k \eta^k \exp(-n\eta), \quad (12)$$

$$\theta(\eta) = \sum_{n=0}^{\infty} \sum_{k=0}^{\infty} b_{m,n}^k \eta^k \exp(-n\eta) \quad (13)$$

where  $a_{m,n}^k$  and  $b_{m,n}^k$  are the coefficients. The appropriate initial approximations and auxiliary linear operators for the considered problems are

$$f_0(\eta) = S + (1 - \exp(-\eta)), \quad \theta_0(\eta) = \exp(-\eta), \quad (14)$$

$$L_f = f''' - f', \quad L_\theta = f'' - f \quad (15)$$

subject to the following properties

$$L_f(C_1 + C_2 e^\eta + C_3 e^{-\eta}) = 0, \quad L_\theta(C_4 e^\eta + C_5 e^{-\eta}) = 0. \quad (16)$$

In which  $C_i$  ( $i = 1-5$ ) denote the arbitrary constants and the zeroth order deformation problems are expressible in the form

$$(1-q)L_f(\hat{f}(\eta; q) - f_0(\eta)) = q\hbar_f \mathbf{N}_f(\hat{f}(\eta; q)), \quad (17)$$

$$(1-q)L_\theta(\hat{\theta}(\eta; q) - \theta_0(\eta)) = q\hbar_\theta \mathbf{N}_\theta(\hat{\theta}(\eta; q), \hat{f}(\eta; q)), \quad (18)$$

$$\hat{f}(0; q) = S, \quad \hat{f}'(0; q) = 1, \quad \hat{f}'(\infty; q) = 0, \quad \hat{\theta}(0; q) = 1 \text{ and } \hat{\theta}(\infty; q) = 0. \quad (19)$$

Here  $q$  shows embedding parameter,  $\hbar_f$  and  $\hbar_\theta$  the non-zero auxiliary parameters and the nonlinear operators  $\mathbf{N}_f$  and  $\mathbf{N}_\theta$  are given by

$$\mathbf{N}_f[\hat{f}(\eta, q)] = \frac{\partial^3 \hat{f}(\eta, q)}{\partial \eta^3} + \hat{f}(\eta, q) \frac{\partial^2 \hat{f}(\eta, q)}{\partial \eta^2} - \left( \frac{\partial \hat{f}(\eta, q)}{\partial \eta} \right)^2 + K_1(x) \left( \frac{\partial^2 \hat{f}(\eta, q)}{\partial \eta^2} \right)^2 \frac{\partial^3 \hat{f}(\eta, q)}{\partial \eta^3} - M^2 \frac{\partial \hat{f}(\eta, q)}{\partial \eta} + K_2(x) \left( \frac{\frac{\partial \hat{f}(\eta, q)}{\partial \eta} \left( \frac{\partial^2 \hat{f}(\eta, q)}{\partial \eta^2} \right)^2 \frac{\partial^3 \hat{f}(\eta, q)}{\partial \eta^3} + \left( \frac{\partial^2 \hat{f}(\eta, q)}{\partial \eta^2} \right)^4 - \hat{f}(\eta, q) \left( \frac{\partial^2 \hat{f}(\eta, q)}{\partial \eta^2} \right)^2 \frac{\partial^4 \hat{f}(\eta, q)}{\partial \eta^4} \right), \quad (20)$$

$$\mathbf{N}_\theta[\hat{\theta}(\eta, q), \hat{f}(\eta, q)] = \left( 1 + \frac{4}{3} N \right) \frac{\partial^2 \hat{\theta}(\eta, q)}{\partial \eta^2} + \varepsilon \hat{\theta}(\eta, q) \frac{\partial^2 \hat{\theta}(\eta, q)}{\partial \eta^2} + \varepsilon \left( \frac{\partial \hat{\theta}(\eta, q)}{\partial \eta} \right)^2 - \text{Pr} \alpha \hat{\theta}(\eta, q) \frac{\partial \hat{f}(\eta, q)}{\partial \eta} + \text{Pr} \hat{f}(\eta, q) \frac{\partial \hat{\theta}(\eta, q)}{\partial \eta}. \quad (21)$$

For  $q = 0$  and  $q = 1$  one has

$$\hat{f}(\eta; 0) = f_0(\eta) \text{ and } \hat{f}(\eta; 1) = f(\eta), \quad (22)$$

$$\hat{\theta}(\eta; 0) = \theta_0(\eta) \text{ and } \hat{\theta}(\eta; 1) = \theta(\eta), \quad (23)$$

and when  $q$  increases from 0 to 1 then  $f(\eta, q)$  and  $\theta(\eta, q)$  vary from  $f_0(\eta)$  to  $f(\eta)$  and  $\theta_0(\eta)$  to  $\theta(\eta)$ . Employing the Taylor's series expansions we have

$$f(\eta, q) = f_0(\eta) + \sum_{m=1}^{\infty} f_m(\eta) q^m, \quad f_m(\eta) = \frac{1}{m!} \left. \frac{\partial^m f(\eta; q)}{\partial \eta^m} \right|_{q=0}, \quad (24)$$

$$\theta(\eta, q) = \theta_0(\eta) + \sum_{m=1}^{\infty} \theta_m(\eta) q^m, \quad \theta_m(\eta) = \frac{1}{m!} \left. \frac{\partial^m \theta(\eta; q)}{\partial \eta^m} \right|_{q=0}. \quad (25)$$

Clearly the convergence of series Eq. (17) and Eq. (18) is closely associated with  $h_f$  and  $h_\theta$ . The values of  $h_f$  and  $h_\theta$  are chosen such that the series Eq. (17) and Eq. (18) converge at  $q = 1$ . Hence

$$f(\eta) = f_0(\eta) + \sum_{m=1}^{\infty} f_m(\eta), \quad (26)$$

$$\theta(\eta) = \theta_0(\eta) + \sum_{m=1}^{\infty} \theta_m(\eta). \quad (27)$$

If we denote the special solutions  $f_m^*$  and  $\theta_m^*$  then the general solutions  $f_m$  and  $\theta_m$  are

$$f_m(\eta) = f_m^*(\eta) + C_1 + C_2 e^\eta + C_3 e^{-\eta}, \quad (28)$$

$$\theta_m(\eta) = \theta_m^*(\eta) + C_4 e^\eta + C_5 e^{-\eta}. \quad (29)$$

### Convergence analysis and discussion

We recall that the auxiliary parameters  $\hbar_f$  and  $\hbar_\theta$  are useful in controlling and adjusting the convergence of series solutions. We draw the  $\hbar$  – curves at 19<sup>th</sup> order of approximation for the meaningful values of  $\hbar_f$  and  $\hbar_\theta$ . It is noticed through **Figures 1** and **2** that the admissible values of  $\hbar_f$  and  $\hbar_\theta$  are  $-0.7 \leq \hbar_f \leq -0.25$  and  $-0.95 \leq \hbar_\theta \leq -0.5$ . Thus our series solutions converge in the whole region of  $\eta$  for  $\hbar_f = -0.5$  and  $\hbar_\theta = -0.7$ .

To see the behaviors of different emerging parameters, we have plotted **Figures 3-14** for the velocity field  $f'(\eta)$  and temperature profile  $\theta(\eta)$ . Variations of  $K_1$ ,  $K_2$ ,  $M$  and  $S$  on the velocity field are depicted in the **Figures 3-6**. Both the non-Newtonian parameters  $K_1$  and  $K_2$  have similar effects on the velocity field in a qualitative sense. By increasing  $K_1$  and  $K_2$  both the velocity and boundary layer thickness increase. It is noticed here that  $K_1$  is negative and  $K_2$  is positive. That is why both parameters have same behaviors. If we take the value of  $K_1$  to be negative then it has opposite behavior as compared to  $K_2$ . Effects of the Hartman number can be seen in **Figure 5**. The Hartman number opposes the flow because the applied magnetic field normal to the flow direction induces the drag in terms of Lorentz force due to which the fluid velocity and boundary layer thickness decreases. **Figure 6** demonstrates the variation of  $S$  on the velocity. Suction is an agent that leads to a decrease in fluid flow due to which the fluid velocity  $f'(\eta)$  decreases by increasing  $S$ . **Figures 7-14** represent the effects of different

parameters on the temperature profile  $\theta(\eta)$ . **Figures 7** and **8** illustrate that temperature and thermal boundary layer thickness are decreasing functions of  $K_1$  and  $K_2$ . Through comparative study of **Figures 3, 4, 7** and **8** we found that the variation in velocity is more significant than the variation in temperature. Hartman number increases the temperature and thermal boundary layer thickness (**Figure 9**). The effects of the Hartman number on velocity and temperature are quite opposite. **Figure 10** illustrates that suction decreases the temperature profile. From **Figures 6** and **10**, we observed that the velocity profile disappears quickly when compared with the temperature. In **Figure 11** we observed that the Prandtl number decreases the thermal boundary layer thickness. In fact an increase in the Prandtl number increases the thermal diffusivity and thus there is a decrease in the temperature profile. By increasing  $\alpha$ , the temperature profile decreases but by increasing  $\varepsilon$  both the temperature and thermal boundary layer thickness increase (**Figure 12**). In addition, an increase in thermal radiation parameter increases the temperature profile and thermal boundary layer thickness. So temperature and thermal boundary layer thickness are decreasing functions of  $N$  (**Figure 13**).

**Table 1** is provided to see how much approximations are required to find a convergent series solution. From this table we see that 15<sup>th</sup> order computations are enough for velocity and 20<sup>th</sup> order computations are sufficient for temperature. It is observed that less computations are required for velocity when compared to temperature. **Table 2** shows the numerical values of skin-friction coefficient for different values of  $K_1$ ,  $K_2$ ,  $M$  and  $S$ . The values of skin-friction coefficient increase by increasing  $S$  and  $M$  and decrease by increasing  $K_1$  and  $K_2$ .

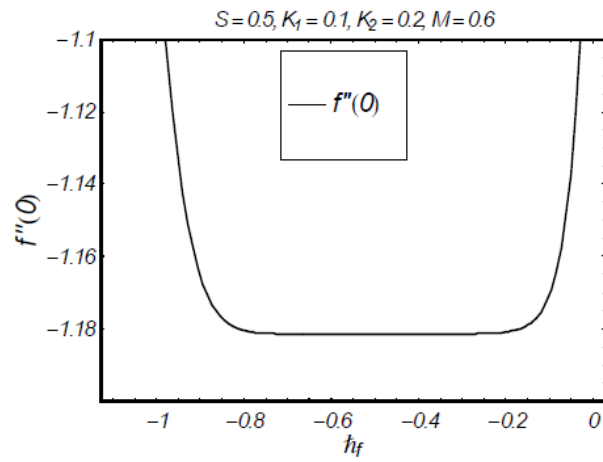


Figure 1  $h$  – curve for the function  $f$  .

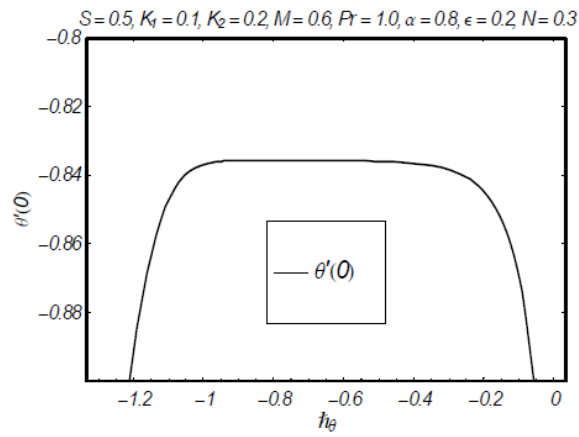


Figure 2  $h$  – curve for the function  $\theta$  .

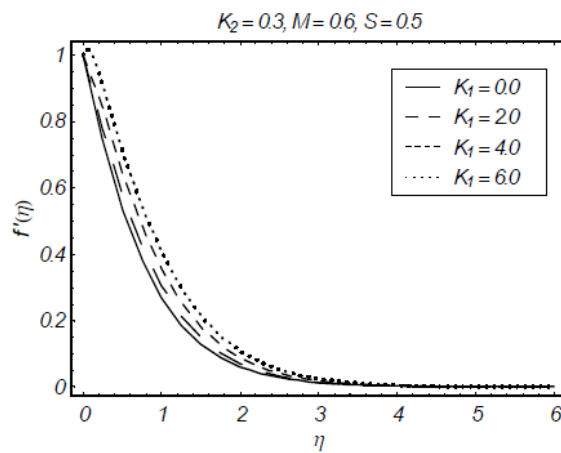


Figure 3 Influence of  $K_1$  on  $f'(\eta)$  .

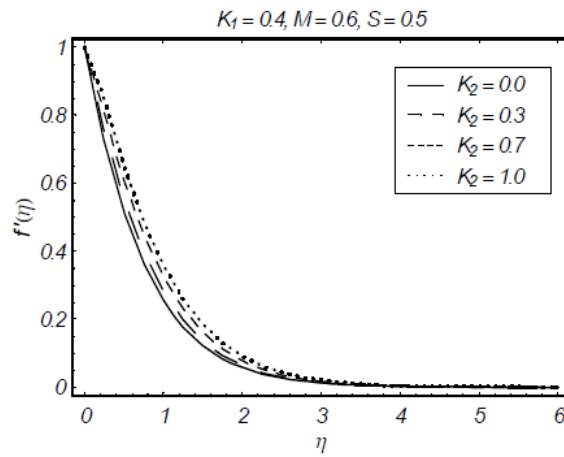


Figure 4 Influence of  $K_2$  on  $f'(\eta)$ .

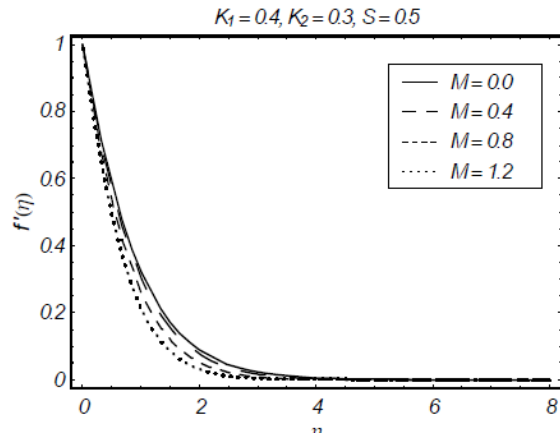


Figure 5 Influence of  $M$  on  $f'(\eta)$ .

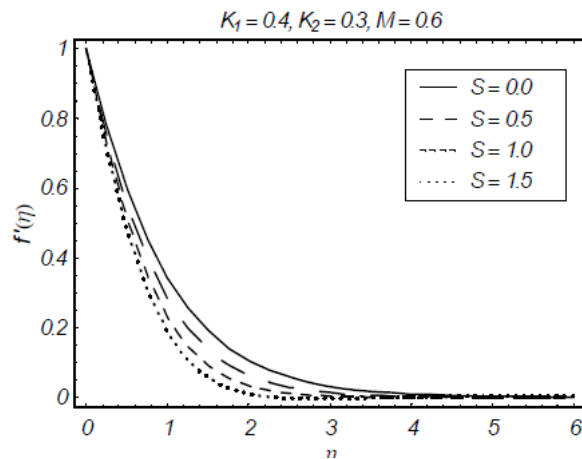


Figure 6 Influence of  $S$  on  $f'(\eta)$ .

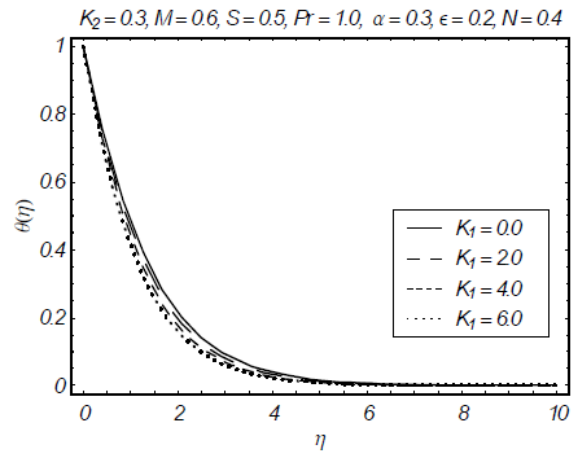


Figure 7 Influence of  $K_1$  on  $\theta(\eta)$ .

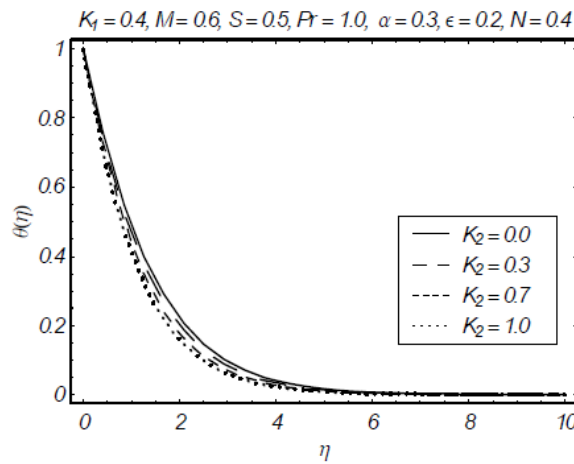


Figure 8 Influence of  $K_2$  on  $\theta(\eta)$ .

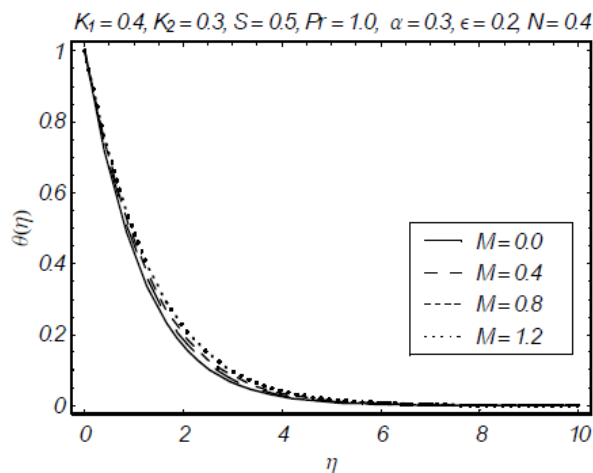
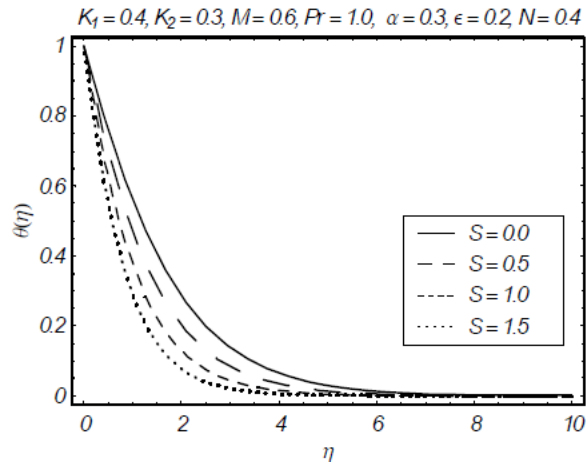
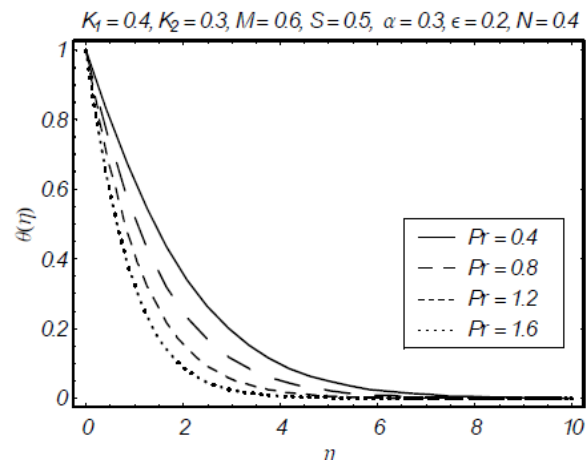


Figure 9 Influence of  $M$  on  $\theta(\eta)$ .



**Figure 10** Influence of  $S$  on  $\theta(\eta)$ .



**Figure 11** Influence of  $Pr$  on  $\theta(\eta)$ .

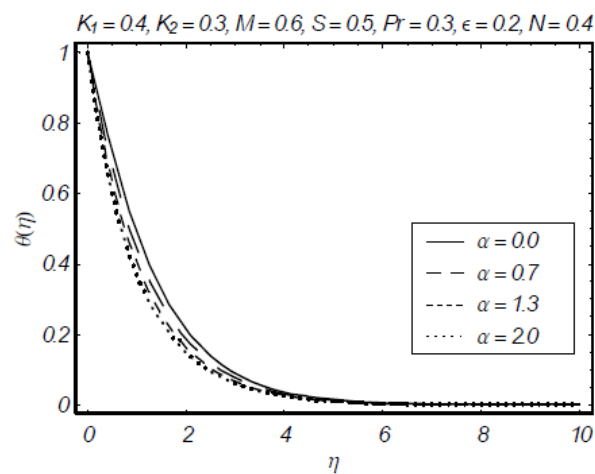


**Figure 12** Influence of  $\alpha$  on  $\theta(\eta)$ .

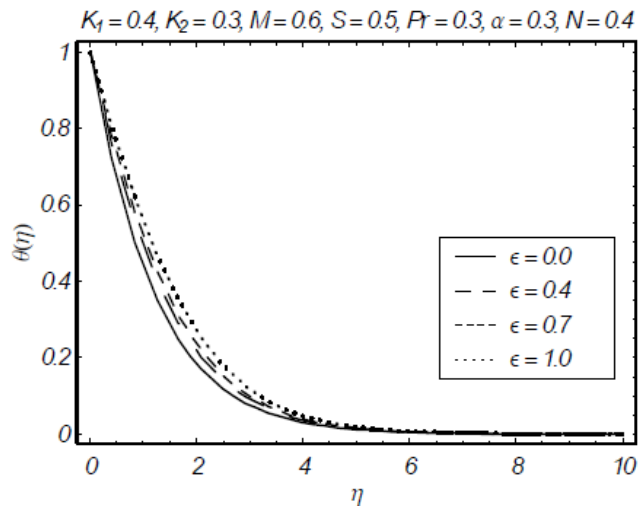


Figure 13 Influence of  $\epsilon$  on  $\theta(\eta)$ .

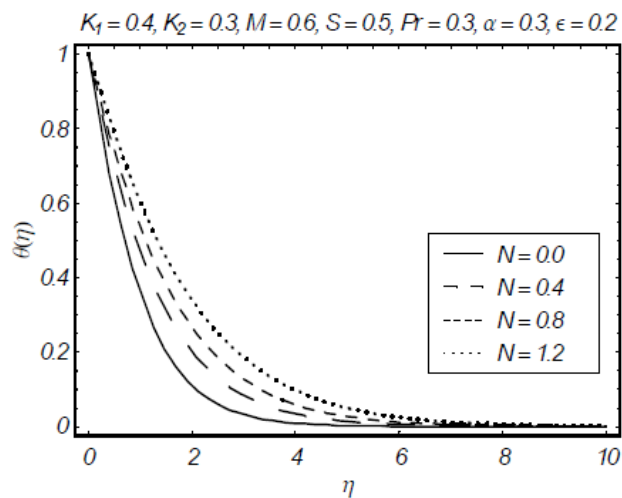


Figure 14 Influence of  $N$  on  $\theta(\eta)$ .

**Table 1** Convergence of series solutions for different order of approximations when  $K_1 = 0.1$ ,  $K_2 = 0.2$ ,  $S = 0.5$ ,  $M = 0.6$ ,  $\varepsilon = 0.2$ ,  $\alpha = 0.8$ ,  $Pr = 1.0$ ,  $N = 0.3$ ,  $\hbar_f = -0.5$  and  $\hbar_0 = -0.8$ .

Order of approximations	$-f''(0)$	$-\theta'(0)$
1	1.12750	0.88000
5	1.18045	0.84353
10	1.18134	0.83659
15	1.18133	0.83583
25	1.18133	0.83572
30	1.18133	0.83572
35	1.18133	0.83572

**Table 2** Numerical values of skin-friction coefficient for different values of  $K_1$ ,  $K_2$ ,  $M$  and  $S$ .

S	M	$K_1$	$K_2$	$-\text{Re}_x^{1/2} C_f$
0.0	0.6	0.1	0.2	1.01988
0.7				1.20293
1.0				1.27055
	0.0			1.05956
	0.4			1.10400
	1.0			1.28407
		0.0		1.20338
		0.5		0.99602
		0.8		0.90599
			0.0	1.33203
			0.4	1.10701
			0.7	1.04074

### Closing remarks

MHD flow of thixotropic fluid over a stretched surface with thermal radiation is studied. Further heat transfer is considered in the presence of variable thermal conductivity. The main results of the conducted study are:

1. The non-Newtonian parameters  $K_1$  and  $K_2$  have quite opposite effects on the velocity and temperature profiles.
2. The effects of  $M$  and  $S$  on the velocity field are similar in a qualitative sense.
3. An increase in  $S$  decreases the temperature and thermal boundary layer thickness.
4. Variations in  $\alpha$  and  $\varepsilon$  on the temperature are quite opposite.
5. The behaviors of  $S$  and  $M$  on the skin friction coefficient are quite opposite to that of  $K_1$  and  $K_2$ .

### References

- [1] A Nejat, A Jalali and M Sharbatdar. A Newton-Krylov finite volume algorithm for the power-law non-Newtonian fluid flow using pseudo-compressibility technique. *J. Non-Newtonian Fluid Mech.* 2011; **166**, 1158-72.
- [2] H Qi and M Xu. Unsteady flow of viscoelastic fluid with fractional Maxwell model in a channel. *Mech. Research Commun.* 2007; **34**, 210-2.
- [3] S Wang and WC Tan. Stability analysis of solet-driven double-diffusive convection of Maxwell fluid in a porous medium. *Int. J. Heat Fluid Flow* 2011; **32**, 88-94.
- [4] M Khan, SH Ali, C Fetecau and Haitao Qi. Decay of potential vortex for a viscoelastic fluid with fractional Maxwell model. *Appl. Math. Modelling* 2009; **33**, 2526-33.
- [5] M Jamil and C Fetecau. Some exact solutions

- for rotating flows of a generalized Burgers' fluid in cylindrical domains. *J. Non-Newtonian Fluid Mech.* 2010; **165**, 1700-12.
- [6] M Jamil and C Fetecau. Helical flows of Maxwell fluid between coaxial cylinders with given shear stresses on the boundary. *Nonlinear Analysis: Real World Appl.* 2010; **11**, 4302-11.
- [7] T Hayat, SA Shehzad, M Qasim and S Obaidat. Steady flow of Maxwell fluid with convective boundary conditions. *Z. Naturforsch A* 2011; **66**, 417-22.
- [8] A Ahmad and S Asghar. Flow of a second grade fluid over a sheet stretching with arbitrary velocities subject to a transverse magnetic field. *Appl. Math. Lett.* 2011; **24**, 1905-9.
- [9] T Hayat, SA Shehzad, M Qasim and S Obaidat. Thermal radiation effects on the mixed convection stagnation-point flow in a Jeffery fluid. *Z. Naturforsch A* 2011; **66**, 606-14.
- [10] K Bhattacharyya, S Mukhopadhyay and GC Layek. Slip effects on an unsteady boundary layer stagnation-point flow and heat transfer towards a stretching sheet. *Chin. Phy. Lett.* 2011; **28**, 09470.
- [11] K Bhattacharyya and GC Layek. Effects of suction/blowing on steady boundary layer stagnation-point flow and heat transfer towards a shrinking sheet with thermal radiation. *Int. J. Heat Mass Transfer* 2011; **54**, 302-7.
- [12] S Nadeem, S Zaheer and T Fang. Effects of thermal radiation on the boundary layer flow of a Jeffery fluid over an exponentially stretching surface. *Numer. Algor.* 2011; **57**, 187-205.
- [13] T Hayat, M Qasim and Z Abbas. Radiation and mass transfer effects on the magnetohydrodynamic unsteady flow induced by a stretching sheet. *Z. Naturforsch A* 2010; **64**, 231-39.
- [14] S Yao, T Fang and J Zhang. Heat transfer of a generalized stretching/shrinking wall problem with convective boundary conditions. *Comm. Nonlinear Sci. Num. Simu.* 2011; **16**, 752-60.
- [15] T Hayat, SA Shehzad, M Qasim and S Obaidat. Radiative flow of Jeffery fluid in a porous medium with power law heat flux and heat source. *Nuclear Eng. Design* 2012; **243**, 15-9.
- [16] S Sadeqi, N Khabazi and K Sadeghy. Blasius flow of thixotropic fluids: A numerical study. *Comm. Nonlinear Sci. Num. Simu.* 2011; **16**, 711-21.
- [17] T Hayat, C Fetecau and M Sajid. Analytic solution for MHD Transient rotating flow of a second grade fluid in a porous space. *Nonlinear Analysis: Real World Appl.* 2008; **9**, 1619-27.
- [18] MM Rashidi and E Erfani. A new analytical study of MHD stagnation-point flow in porous media with heat transfer. *Comput. Fluids* 2011; **40**, 172-8.
- [19] M Turkyilmazoglu. Unsteady MHD flow with variable viscosity: Applications of spectral scheme. *Int. J. Thermal Sci.* 2010; **49**, 563-70.
- [20] OD Makinde and T Chinyoka. MHD transient flows and heat transfer of dusty fluid in a channel with variable physical properties and Navier slip condition. *Comput. Math. Appl.* 2010; **60**, 660-9.
- [21] S Abbasbandy and T Hayat. Solution of the MHD Falkner-Skan flow by homotopy analysis method. *Commun. Nonlinear Sci. Numer. Simulat.* 2009; **14**, 3591-8.
- [22] T Hayat, FM Abbasi and S Obaidat. Peristaltic motion with Soret and Dufour effects. *Magnetohydrodynamics* 2011; **47**, 295-302.
- [23] WM Kay. Convective heat and mass transfer, *Mc-Graw Hill, New York*, 1996.
- [24] P Vyas and A Rai. Radiative flow with variable thermal conductivity over a non-isothermal stretching sheet in a porous medium. *Int. J. Contemp. Math. Sciences* 2010; **5**, 2685-98.
- [25] SJ Liao. Beyond perturbation: Introduction to homotopy analysis method. *Chapman and Hall, CRC Press, Boca Raton*, 2003.
- [26] H Vosughi, E Shivanian and S Abbasbandy. A new analytical technique to solve Volterra's integral equations. *Math. Methods Appl. Sci.* 2011; **34**, 1243-53.
- [27] MM Rashidi and SAM Pour. Analytic approximate solutions for unsteady boundary-layer flow and heat transfer due to a stretching sheet by homotopy analysis method. *Nonlinear Anal. Model. Contr.* 2010; **15**, 83-95.
- [28] B Yao. Approximate analytical solution to

- the Falkner-Skan wedge flow with the permeable wall of uniform suction. *Commun. Nonlinear Sci. Numer. Simulat.* 2009; **14**, 3320-6.
- [29] MM Rashidi, SAM Pour and S Abbasbandy. Analytic approximate solutions for heat transfer of a micropolar fluid through a porous medium with radiation. *Commun. Nonlinear Sci. Numer. Simulat.* 2011; **16**, 1874-89.
- [30] T Hayat, SA Shehzad and M Qasim. Mixed convection flow of a micropolar fluid with radiation and chemical reaction. *Int. J. Num. Methods Fluids* 2011; **67**, 1418-36.